Mechanism of H_2S-mediated protection against oxidative stress in *Escherichia coli*

Alexander Mironov[a,b], Tatyana Seregina[b], Maxim Nagornykh[b], Lyly G. Luhachack[c], Natalya Korolkova[a], Liubov Errais Lopes[a], Vera Kotova[a], Gennady Zavilgelsky[a], Rustem Shakulov[a], Konstantin Shatalin[c], and Evgeny Nudler[c,d,1]

[a]Department of Genetics, State Research Institute of Genetics and Selection of Industrial Microorganisms, Moscow 117545, Russia; [b]Department of Molecular Biology, Engelhardt Institute of Molecular Biology, Russian Academy of Science, Moscow 119991, Russia; [c]Department of Biochemistry and Molecular Pharmacology, New York University School of Medicine, New York, NY 10016; and [d]Howard Hughes Medical Institute, New York University School of Medicine, New York, NY 10016

Edited by James J. Collins, Massachusetts Institute of Technology, Boston, MA, and approved April 27, 2017 (received for review March 3, 2017)

Endogenous hydrogen sulfide (H_2S) renders bacteria highly resistant to oxidative stress, but its mechanism remains poorly understood. Here, we report that 3-mercaptopyruvate sulfurtransferase (3MST) is the major source of endogenous H_2S in *Escherichia coli*. Cellular resistance to H_2O_2 strongly depends on the activity of *mstA*, a gene that encodes 3MST. Deletion of the ferric uptake regulator (Fur) renders Δ*mstA* cells hypersensitive to H_2O_2. Conversely, induction of chromosomal *mstA* from a strong pLtetO-1 promoter (P_{tet}-*mstA*) renders Δ*fur* cells fully resistant to H_2O_2. Furthermore, the endogenous level of H_2S is reduced in Δ*fur* or Δ*sodA* Δ*sodB* cells but restored after the addition of an iron chelator dipyridyl. Using a highly sensitive reporter of the global response to DNA damage (SOS) and the TUNEL assay, we show that 3MST-derived H_2S protects chromosomal DNA from oxidative damage. We also show that the induction of the CysB regulon in response to oxidative stress depends on 3MST, whereas the CysB-regulated L-cystine transporter, TcyP, plays the principle role in the 3MST-mediated generation of H_2S. These findings led us to propose a model to explain the interplay between L-cysteine metabolism, H_2S production, and oxidative stress, in which 3MST protects *E. coli* against oxidative stress via L-cysteine utilization and H_2S-mediated sequestration of free iron necessary for the genotoxic Fenton reaction.

hydrogen sulfide | oxidative stress | cysteine | sulfur metabolism | antibiotics

Hydrogen sulfide (H_2S) is well-recognized as a second messenger implicated in many physiological processes in mammals, including synaptic transmission, vascular tone, inflammation, angiogenesis, and protection from oxidative stress (1). The latter function of H_2S seems to be universal, because it has been implicated in bacterial defense against reactive oxygen species (ROS) and antibiotics-induced oxidative damage (2). H_2S can also kill microorganisms by inhibiting antioxidant enzymes during induced oxidative stress (3, 4). These seemingly contradictory attributes of H_2S highlight its concentration-dependent dual nature: at high concentration, it is a toxic gas, and at lower physiological concentrations, it is a signaling and/or protective molecule.

In *Escherichia coli* grown in Luria–Bertani broth, 3-mercaptopyruvate sulfurtransferase (3MST) is responsible for the bulk of endogenous H_2S generated from L-cysteine (2). Although *E. coli* has several known L-cysteine desulfhydrases (CDs), including *O*-acetylserine sulfhydrylases A and B (CysK and CysM), cystathionine β-lyases A and B (MetC and MalY), and tryptophanase (TnaA), that can, in principle, generate H_2S as a by-product of L-cysteine degradation, their contribution to H_2S production under normal growth conditions has not been established (2, 5). Because L-cysteine can be toxic to bacteria (6, 7), its intracellular level is tightly controlled. Excess L-cysteine inhibits the activity of L-serine *O*-acetyltransferase, a key enzyme in the L-cysteine biosynthetic pathway (8). The LysR-type transcriptional regulator, CysB, controls expression of genes involved in cysteine biosynthesis and sulfur assimilation. CysB binds the inducer, *N*-acetyl-L-serine (NAS), the product of a nonenzymatic rearrangement of *O*-acetyl-L-serine (OAS) that activates its binding to promoter DNA sequences (9). It has been shown that a high level of intracellular L-cysteine promotes the Fenton reaction (10):

$$\text{L-cysteine} + Fe^{3+} \rightarrow \text{L-cystine} + Fe^{2+}$$

$$Fe^{2+} + H_2O_2 \rightarrow Fe^{3+} + \cdot OH + OH^-.$$

This process is potentially toxic to the cell, because the resulting hydroxyl radicals damage nucleic acids, carbonylate proteins, and peroxidate lipids (11–13).

In our previous experiments, we showed in various bacterial species that an exogenous H_2S donor could suppress H_2O_2-mediated DNA damage (2). Here, we extend these findings to show that 3MST-mediated endogenous production of H_2S suppresses oxidative stress in *E. coli* by sequestering free iron required to drive the genotoxic Fenton reaction. Furthermore, we elucidate the complex interplay between 3MST and the CysB regulon that controls intracellular L-cysteine as a rate-limiting factor in H_2O_2-driven cytotoxicity.

Results

3MST-Derived H_2S Protects *E. coli* from H_2O_2 by Sequestering Free Iron. To study the biochemistry of endogenous H_2S in *E. coli* and determine whether it is cytoprotective against ROS, we

Significance

Hydrogen sulfide (H_2S) is a highly toxic gas that interferes with cellular respiration; however, at low physiological amounts, it plays an important role in cell signaling. Remarkably, in bacteria, endogenously produced H_2S has been recently recognized as a general protective molecule, which renders multiple bacterial species highly resistant to oxidative stress and various classes of antibiotics. The mechanism of this phenomenon remains poorly understood. In this paper, we use *Escherichia coli* as a model system to elucidate its major enzymatic source of H_2S and establish the principle biochemical pathways that account for H_2S-mediated protection against reactive oxygen species. Understanding those mechanisms has far-reaching implications in preventing bacterial resistance and designing effective antimicrobial therapies.

Author contributions: A.M. and E.N. designed research; A.M., T.S., M.N., L.G.L., N.K., L.E.L., V.K., and K.S. performed research; G.Z. and R.S. contributed new reagents/analytic tools; A.M., T.S., M.N., L.G.L., G.Z., R.S., and K.S. analyzed data; and A.M. and E.N. wrote the paper.

The authors declare no conflict of interest.

This article is a PNAS Direct Submission.

[1]To whom correspondence should be addressed. Email: evgeny.nudler@nyumc.org.

This article contains supporting information online at www.pnas.org/lookup/suppl/doi:10.1073/pnas.1703576114/-/DCSupplemental.

generated *E. coli* strains either lacking a chromosomal copy of the 3MST-encoding gene *mstA* (also known as *sseA*) or carrying it under a strong pLtetO-1 promoter (P_{tet}-*mstA*). After induced, P_{tet}-derived 3MST should remain at a constantly high level. We used two complementary methods to quantify the level of H_2S production by *E. coli* cells (Fig. 1). The first method is based on the specific reactivity of lead acetate [$Pb(Ac)_2$] with H_2S, resulting in a brown lead sulfide stain. The rate of staining on a $Pb(Ac)_2$-soaked paper strip is directly proportional to the concentration of H_2S (14). The second method uses the twister internal charge transfer (TICT)-based fluorescent probe for H_2S (15). The TICT probe is cell-permeable and allows for monitoring exogenous and endogenous H_2S in living cells. Both methods consistently show that 3MST-deficient *E. coli* exhibit reduced level of H_2S production, whereas P_{tet}-*mstA* cells produce much more H_2S compared with the WT (Fig. 1).

Next, we examined the sensitivity of those cells to peroxide. H_2O_2 was added to midlog phase cultures ($OD_{600} \sim 0.2$) at time 0, and the percentages of viable cells in the population were measured at intervals of 10, 20, and 30 min (Fig. 2*A*). After 20 min of treatment with 2 mM H_2O_2, the viabilities of WT and *ΔmstA* cells were reduced by ∼10 and 25%, respectively. P_{tet}-*mstA* cells displayed no loss of viability (Fig. 2*A*). Notably, the exposure of WT cells to peroxide stimulated H_2S production (Fig. 1*B*), indicating that cells respond to oxidative stress by stimulating the activity of 3MST.

H_2O_2 is only mildly genotoxic to WT K-12 *E. coli*, which contains little free iron (16). We, therefore, sought to promote Fenton chemistry by elevating intracellular free iron in all three strains. Ferric uptake regulator (Fur) is the master transcriptional regulator of iron uptake and homeostasis in *E. coli* (17, 18). For example, Fur represses a small RNA RyhB, which negatively regulates a number of iron-containing proteins in *E. coli* (19). Fur deletion results in a constitutive import of iron (20, 21) and hypersensitivity to oxidative DNA damage (22). Accordingly, inactivation of *fur*, with or without *ryhB*, resulted in a 40-fold

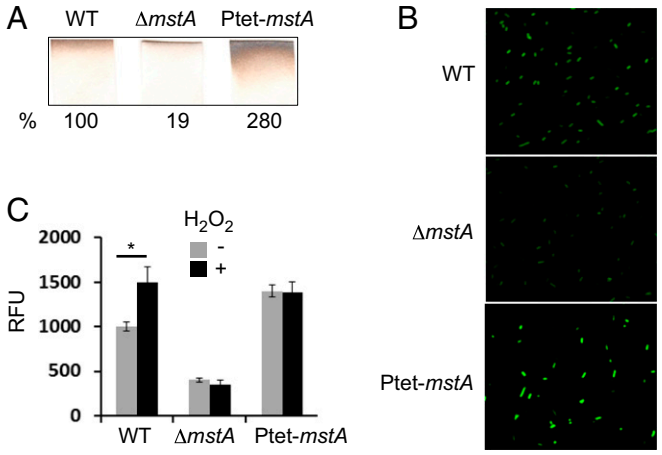

Fig. 1. Quantitation of H_2S production by WT, 3MST-deficient (Δ*mstA*), and 3MST-overproducing (P_{tet}-*mstA*) *E. coli*. (*A*) Representative $Pb(Ac)_2$-soaked paper strips show a PbS brown stain as a result of the reaction with H_2S. Strips were affixed to the inner wall of a culture tube above the level of the liquid culture of WT or mutant bacteria for 18 h. Numbers show the change in H_2S production relative to WT cells. The values are means from three independent experiments with a margin error of less than 10%. (*B*) Representative fluorescence images of H_2S production by live WT and mutant *E. coli* cells treated with the TICT-based fluorescent H_2S probe (15). (Magnification: 100×.) (*C*) Fluorescence intensities of WT and mutant *E. coli* cells in Luria–Bertani broth or Luria–Bertani broth plus 2 mM H_2O_2 treated with fluorescent H_2S probe as detected by Cytation 3 (BioTek Instruments Inc.). Values are means ± SD ($n = 3$). RFU, relative fluorescence unit. *$P < 0.05$ (Student's *t* test; equal variance).

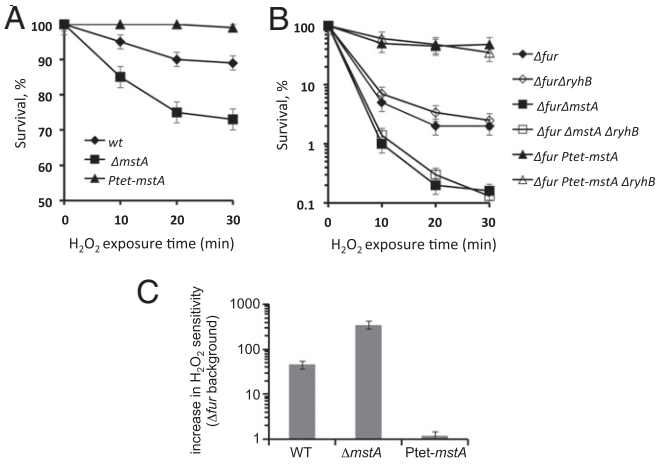

Fig. 2. 3MST-derived H_2S protects *E. coli* from H_2O_2 toxicity. (*A*) Representative survival curves show the effect of H_2S deficiency (Δ*mstA*) or overproduction (P_{tet}-*mstA*) on H_2O_2-mediated killing. (*B*) An *fur* mutation promotes H_2O_2 cytotoxicity in WT and Δ*mstA* cells but not in P_{tet}-*mstA* cells. The percentage of surviving cells was determined by counting cfu and is shown as the mean ± SD from three experiments. (*C*) Relative change in H_2O_2 sensitivity of WT, Δ*mstA*, and P_{tet}-*mstA* cells in response to Fur deficiency (Δ*fur*). Values are means ± SD from three experiments.

increase in cell death from H_2O_2 (Fig. 2 *B* and *C*). The survivability of *Δfur*, or *Δfur ΔryhB*, cells deficient in H_2S production (Δ*mstA*) decreased much more drastically (∼360-fold). In contrast, Δ*fur*, or *Δfur ΔryhB*, cells that overproduced H_2S (P_{tet}-*mstA*) displayed almost complete loss of susceptibility to H_2O_2 (Fig. 2 *B* and *C*), suggesting that H_2S counteracts the toxicity of H_2O_2 by sequestering the excess of free iron in Fur-deficient cells.

In support of this conclusion, we showed that the addition of $FeCl_3$ reduces the amount of H_2S in P_{tet}-*mstA* cells (Fig. 3*A*). We also observed a significant H_2S reduction in P_{tet}-*mstA* cells deleted of *fur* or *sodA*/*sodB* (Fig. 3*A*). The levels of free chelatable iron in *Δfur* and Δ*sodA*/*sodB* mutants and the triple *Δfur* Δ*sodA* Δ*sodB* mutant are ∼8- and 17-fold higher, respectively, compared with WT cells (21). Accordingly, we observed the largest decrease in detectable H_2S in P_{tet}-*mstA* cells in the *Δfur* Δ*sodA* Δ*sodB* mutant (Fig. 3*A*). Moreover, addition of an iron chelator, 2,2′-dipyridyl, fully restored the high level of H_2S in all P_{tet}-*mstA* strains (Fig. 3*A*). Because the inactivation of *fur* or *sodA*/*sodB* did not affect the level of *mstA* gene expression (Fig. S1), we conclude that the level of H_2S generated by 3MST is inversely proportional to the level of intracellular free iron. Taken together, these results argue that endogenous H_2S protects against H_2O_2-mediated toxicity by directly sequestrating Fe^{2+}.

3MST Is the Major CD That Protects Genomic DNA from Oxidative Damage. Formation of double-strand breaks (DSBs) in DNA is the primary cause of bacterial cell death resulting from exposure to peroxide (23). These DSBs are the result of the toxic effects of the hydroxyl radical generated by the Fenton reaction (24). To examine whether endogenous H_2S protects bacteria from DNA damage caused by the Fenton reaction, we first examined its effect on the global response to DNA damage (SOS). We used a pColD′::lux reporter plasmid to directly monitor SOS activation in response to DNA damage (25). Fig. 3*B* shows the bioluminescence induction curves as a function of H_2O_2 concentrations in *Δfur*, *Δfur* Δ*mstA*, and *Δfur* P_{tet}-*mstA* cells carrying pColD′::lux. In *Δfur* cells, SOS induction begins at a concentration of 5 μM H_2O_2 and reaches a maximum at 80 μM followed by the decrease of bioluminescence caused by cell death. The *Δfur* Δ*mstA* mutant exhibits a maximal SOS response at the lower concentration of H_2O_2

BIOCHEMISTRY

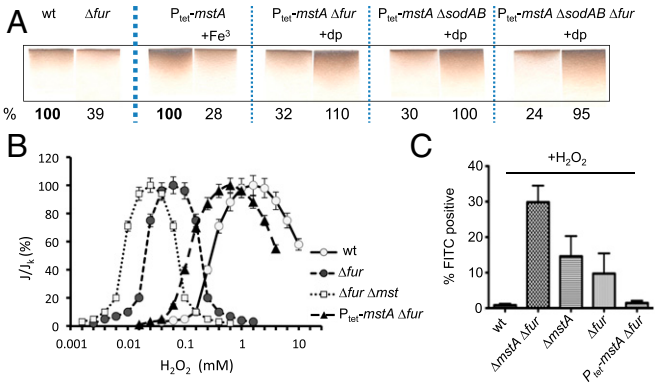

Fig. 3. 3MST-derived H_2S protects genomic DNA from the damaging Fenton reaction. (*A*) 3MST-derived H_2S sequesters intracellular iron. Representative $Pb(Ac)_2$-soaked paper strips show the decrease in the amount of H_2S generated in P_{tet}-*mstA* cells in response to deletion of *fur* or *sodA sodB* genes. Such deletions cause a drastic increase in the intracellular free iron content (21). Addition of 200 μM 2,2′-dipyridyl (dp), an iron chelator, restores H_2S to its original level in each case. The values (percentages) are means from three independent experiments with a margin error of less than 10%. (*B*) 3MST-derived H_2S renders cells less susceptible to DNA damage as evidenced by the higher H_2O_2 concentration necessary to induce the SOS response in P_{tet}-*mstA* cells. The SOS response was monitored by bioluminescence of the lux biosensor (pColD′::lux) in *Δfur*, *Δfur ΔmstA*, *Δfur* P_{tet}-*mstA*, and WT cells in the presence of different concentrations of H_2O_2. J/J_k indicates the induction factor in percentage compared with the maximal intensity of bioluminescence of samples in the presence of H_2O_2. Values are means ± SD from three experiments. (*C*) 3MST-derived H_2S renders cells less susceptible to H_2O_2-induced DNA breaks as detected by TUNEL. The graph shows the percentage of gated propidium iodide cells that are TUNEL-positive as detected by fluorescence intensity greater than that of untreated cells. Statistical evaluation (one-way ANOVA and Tukey's post hoc test) was performed to evaluate differences in the cell population.

(40 μM). In contrast, Δ*fur* P_{tet}-*mstA* cells reach the peak of bioluminescence intensity at a much higher H_2O_2 concentration (~1 mM), which is similar to that of the WT (Fig. 3*B*). These data indicate that endogenous H_2S significantly augments cellular tolerance to the Fenton reaction.

To further assess DNA damage after H_2O_2 treatment, we used an assay in which 3′-OH DNA ends were labeled with TUNEL followed by analysis by flow cytometry (Fig. 3*C* and Fig. S2). The percentage of TUNEL-positive cells, after gating for propidium iodide-stained cells, was significantly higher in *Δfur ΔmstA* than WT or *Δfur* P_{tet}-*mstA* cells. However, there was no significant difference in the percentages of TUNEL-positive cells between treated WT and *Δfur* P_{tet}-*mstA* cells. Moreover, at the 5 mM concentration of H_2O_2, the threshold of detection for TUNEL-positive cells is minimal for WT and *Δfur* P_{tet}-*mstA*–treated cells. These results show directly that endogenous H_2S effectively protects chromosomal DNA from H_2O_2-induced DSBs.

The high level of resistance to oxidative stress observed in P_{tet}-*mstA* cells may not be only caused by the efficient sequestration of free iron but also, may be because of a higher rate of L-cysteine utilization via the sequential action of aspartate aminotransferase (AspC) and 3MST. L-cysteine promotes the Fenton reaction by effectively reducing Fe^{3+} to Fe^{2+} (10). Therefore, the intensive L-cysteine degradation in P_{tet}-*mstA* cells can also contribute to the suppression of the Fenton reaction.

E. coli has five known CDs in addition to 3MST, which are capable of degrading L-cysteine to pyruvate, ammonia, and sulfide. However, a quintuple mutant of Δ*tnaA* Δ*metC* Δ*cysK* Δ*cysM* Δ*malY* retains significant CD activity, which is increased in the presence of L-cysteine (5), suggesting that the major enzyme responsible for converting L-cysteine to H_2S is 3MST. Indeed, 3MST is not only responsible for the bulk of H_2S during normal growth in rich media but also, generates more H_2S under exposure to peroxide (Fig. 1*C*). In contrast, TnaA, which is considered to be the predominant CD (5), contributes little to the overall level of endogenous H_2S (Fig. S3*A*) and does not influence bacterial susceptibility to H_2O_2, irrespective of Fur (Fig. S3*B*).

Functional Interaction Between 3MST and CysB. CysB is a master transcriptional regulator of sulfur metabolism that senses the level of endogenous L-cysteine (8). To further evaluate the impact of 3MST on endogenous L-cysteine catabolism, we used quantitative RT-PCR (qRT-PCR) to measure the expression of the CysB-dependent genes, *cysK*, *cysP*, and *tau*, in *ΔmstA* and P_{tet}-*mstA* cells. Transcription of all three genes was mildly decreased in *ΔmstA* cells compared with WT cells (Fig. 4*A*). In P_{tet}-*mstA* cells, however, *cysK*, *cysP*, and *tau* were induced ~11-, 8-, and 5-fold, respectively. The induction of these genes is strictly dependent on CysB, because *cysB* inactivation reduced their expression to the background level (Fig. 4*A*). We infer that the induction of CysB-dependent genes was caused by the induction of *cysB* itself (Fig. 4*A*), which is likely to occur because of the increased L-cysteine degradation in P_{tet}-*mstA* cells. Indeed, L-cysteine is involved in feedback inhibition of serine acetyltransferase, CysE, which generates OAS, a precursor of an autoinducer for CysB, NAS (Fig. S4) (9). Accordingly, the addition of exogenous L-cysteine to the Ptet-*mstA* strain reduced the expression of all CysB-regulated genes to the basal level (Fig. 4*A*).

We next examined the effect of 3MST on the CysB regulon during oxidative stress. Treatment of WT cells with 2 mM H_2O_2 for 20 min resulted in 5-, 23-, 10-, and 14-fold inductions of *cysB*, *cysK*, *cysP*, and *tau*, respectively (Fig. 4*B*). In contrast, the induction of CysB-regulated genes in response to H_2O_2 was completely abolished in *ΔmstA* cells (Fig. 4*B*), showing the principle role of 3MST-derived H_2S in CysB-dependent gene regulation in response to stress. Notably, the deletion or overexpression of *tnaA* had no effect on transcription of CysB-regulated genes (Fig. S5).

The reciprocal communication between CysB and 3MST is further evident from the requirement of CysB for H_2S-mediated protection against oxidative stress. Inactivation of *cysB* increased the sensitivity of Δ*fur* cells to H_2O_2, which cannot be suppressed by P_{tet}-*mstA* (Fig. S6). Moreover, inactivation of *cysB* almost completely abolished H_2S generation by P_{tet}-*mstA* cells (Fig. 5*A*). We suggest that, without CysB, the transport of L-cysteine into

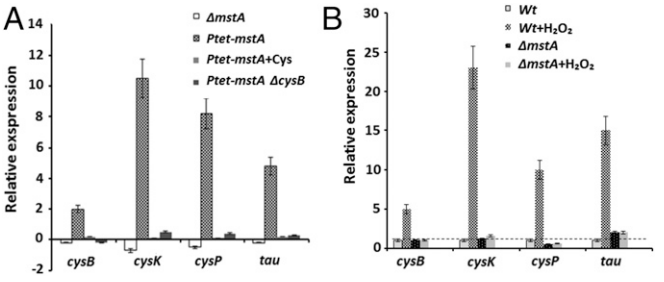

Fig. 4. Functional interaction between 3MST and CysB regulon. (*A*) The relative expression of CysB-regulated genes in exponentially grown *ΔmstA* and P_{tet}-*mstA* cells was measured by qRT-PCR. The relative expression (*y* axis) represents the fold change of each mRNA level compared with that of the untreated cells. Values are means ± SD from four experiments. (*B*) Induction of CysB-regulated gene expression by H_2O_2 (2 mM, 20 min) in exponentially grown WT and *ΔmstA* cells as detected by qRT-PCR. The relative expression (*y* axis) represents the fold change of each mRNA level after treatment of the cells with H_2O_2 compared with that of the untreated cells (dashed line). Values are means ± SD from four experiments.

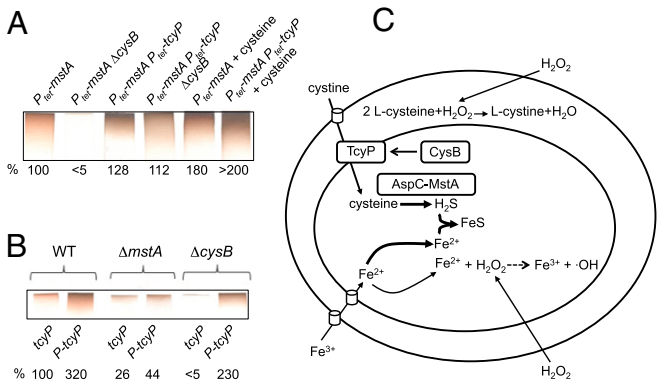

Fig. 5. Interdependence between 3MST activity and L-cysteine/cystine import. Constitutive expression of the TcyP transporter suppresses the negative effect of *cysB* deletion on H_2S production in (*A*) P_{tet}-*mstA* cells or (*B*) Δ*mstA* and WT cells as detected by the $Pb(Ac)_2$ assay. Representative panels show mean values (percentages) from three independent experiments with a margin error of less than 10%. (*C*) A model of H_2S-mediated defense against oxidative stress in *E. coli*. A fraction of exogenous H_2O_2 reacts with L-cysteine in the periplasm to form L-cystine and H_2O. This reaction leads to a decrease in the intracellular content of L-cysteine with a subsequent relief of autoregulation of *cysB* and activation of CysB-dependent genes, including *tcyP*, which is responsible for transport of L-cystine into the cell. Overflow of cystine/cysteine flux results in increased *mstA*-dependent generation of H_2S, which sequesters free iron to prevent the Fenton reaction and formation of damaging hydroxyl radicals.

the cell is abrogated, hence the inability of 3MST to generate H_2S and protect against oxidative stress.

To test this hypothesis, we placed the chromosomal copy of the major L-cystine importer, *tcyP* (26, 27), under the strong Ptet promoter. TcyP is normally under the positive control of CysB (28). Ptet-*tcyP* fully restored 3MST-dependent H_2S production in Ptet-*mstA* cells (Fig. 5*A*). Moreover, Ptet-*tcyP* increased H_2S production in *cysB*(−) or (+) cells carrying *mstA* under its native promoter (Fig. 5*B*). Because the deletion of *mstA* in Ptet-*tcyP* cells abolishes H_2S production, we conclude that 3MST is the sole source of H_2S in *E. coli* grown in Luria–Bertani broth. These results argue that, under conditions of cystine overflow, the AspC-3MST system generates a sufficient amount of H_2S to render cells resistant to oxidative stress. To maintain such a protective level of H_2S under oxidative stress, the enhanced influx of L-cysteine must occur. Accordingly, the expression of *tcyP* is strongly induced in response to H_2O_2 treatment (Fig. S7). Moreover, this induction is strictly dependent of 3MST activity: deletion of *mstA* abolishes *tcyP* induction, whereas Ptet-*mstA* increases it (Fig. S7).

Discussion

The purpose of this work is to explain the mechanism of H_2S-mediated protection against oxidative stress and establish the biochemical pathway of H_2S production in response to stress in *E. coli*. The results determine that the AspC-3MST pathway is the principle source of H_2S in *E. coli* grown in rich medium containing cysteine (Fig. S4). It has been assumed that TnaA could be the major CD and potential generator of H_2S in *E. coli* (5). However, our previous work showed that inactivation of TnaA (Δ*tnaA*) or other known desulfhydrases (Δ*metC*, Δ*cysK*, Δ*cysM*, and Δ*malY*) does not significantly alter the level of endogenous H_2S (2). Here, we provide independent support for this conclusion and show that the inactivation or overexpression of TnaA does not function at all in H_2S-mediated protection against oxidative stress (Fig. S3). Rather, 3MST is central.

The protective function of 3MST becomes most apparent in Fur-deficient cells, in which the level of intracellular iron (Fe^{2+}) substantially increased (22). The Δ*mstA* Δ*fur* double mutant exhibited a 360-fold increase in sensitivity to H_2O_2 compared with its Δ*mstA fur*$^+$ counterpart (Fig. 2), which showed an ∼10-fold increase in peroxide sensitivity compared with the Δ*fur* mutant. This sensitivity correlates well with the dramatic increase in genomic DNA DSBs (Fig. 3*C* and Fig. S2). Remarkably, endogenous overproduction of H_2S from the chromosomal Ptet-*mstA* completely protects Fur-deficient cells from H_2O_2 toxicity and DNA damage. Furthermore, we found that the level of H_2S in P_{tet}-*mstA* cells is reduced in Δ*fur* or Δ*sodA* Δ*sodB* cells but can be restored after addition of the FE^{2+} chelator, 2,2′-dipyridyl (Fig. 3*A*). These data imply that 3MST renders *E. coli* resistant to oxidative stress via H_2S-mediated sequestration of Fe^{2+}, thereby diminishing the genotoxic Fenton reaction (Fig. 5*C*).

Because the amino acids in Luria–Bertani broth are the main carbon source (29), we postulate that Luria–Bertani broth-derived L-cystine/cysteine is the principle substrate for H_2S production by AspC-3MST. Indeed, the deletion of *cysB* abolishes the generation of H_2S in P_{tet}-*mstA* cells. CysB positively regulates not only the genes responsible for L-cysteine biosynthesis but also, *tcyP* and *tcyJ*, which encode the two L-cystine transporters, the symporter TcyP and the ATP binding cassette importer TcyJ, respectively (27). Therefore, the inability of the Ptet-*mstA* Δ*cysB* mutant to generate H_2S can be caused by reduced production of endogenous L-cysteine, disruption of L-cystine import from the Luria–Bertani broth medium, or both. We found that the introduction of the constitutively active form of *tcyP* (Ptet-*tcyP*) (Fig. 5*A*), but not *tcyJ* (Ptet-*tcyJ*) (Fig. S8), fully restores the generation of H_2S in CysB-deficient Ptet-*mstA* cells. Remarkably, we found that the constitutive expression of *tcyP* also leads to overproduction of H_2S in cells with native expression of *mstA* (Fig. 5*B*). Thus, the main source of H_2S generated by 3MST is L-cystine/cysteine imported from the Luria–Bertani broth medium by the TcyP transporter (Fig. 5*C*). This conclusion is consistent with the observation that, unlike TcyJ, TcyP functions predominantly as a nutrient importer under normal growth conditions (26).

Our results also reveal the reciprocal interaction between 3MST and the CysB regulon under normal growth conditions and during oxidative stress. The high level of 3MST expression in Ptet-*mstA* cells resulted in *cysB* induction and its target genes (*cysK*, *cysP*, and *tau*), whereas in the absence of 3MST, the expression of all CysB-regulated genes was diminished (Fig. 4*A*). Remarkably, 3MST deficiency also abolished H_2O_2-mediated induction of CysB-dependent genes (Fig. 4*B*). It has been reported that at least three such genes (*cysK*, *cysP*, and *tcyJ*) are highly up-regulated in response to H_2O_2 in an OxyR-independent manner (26, 30). The mechanism of such an induction remains unknown. Our results suggest the following model, which explains the interplay between oxidative stress, activation of the CysB regulon, and 3MST-dependent generation of H_2S (Fig. 5*C*). The sulfhydryl group of L-cysteine reacts with H_2O_2 in the periplasm to yield L-cystine (26). This reaction lowers the intracellular level of L-cysteine leading to the induction of the CysB regulon, including the TcyP transporter, thereby boosting the L-cystine/cysteine influx into the cytoplasm. The increased flow of L-cysteine stimulates H_2S production by the AspC-3MST pathway, leading to sequestration of Fe^{2+} and suppression of the Fenton reaction (Fig. 5*C*). Inactivation of 3MST halts the conversion of L-cysteine to H_2S, leading to accumulation of intracellular L-cysteine, thereby preventing H_2O_2-dependent induction of CysB-regulated genes and fueling the genotoxic Fenton reaction.

Understanding the mechanism of H_2S-mediated protection against ROS has important implications for bacterial resistance to antibiotics (31, 32). Pharmacological inhibition of bacterial H_2S production may facilitate rapid bacterial killing, which would not only widen the therapeutic window for many classes of

bactericidal antibiotics but also, diminish the rate at which bacteria acquire resistance to such antibiotics (33).

Materials and Methods

Strains and Growth Conditions. All *E. coli* strains used in this work are listed in Table S1. BW25113 and its derivatives (single-gene deletion mutants) were obtained from the *E. coli* Keio Knockout Collection (Thermo Scientific) (34). Details of strain constructions are described in *SI Materials and Methods*. P1 transduction was used to introduce mutations into new strains (35). When necessary, Cam or Kan drug resistance markers were excised from strains using the flippase activity of pCP20 followed by loss of the plasmid at nonpermissive temperature (36). All mutations were verified by PCR and gel analysis. DNA manipulations and the transformation of *E. coli* strains were performed according to standard methods (37). Luria–Bertani broth complete medium was used for the general cultivation of *E. coli*. When appropriate, antibiotics were added at 40 μg/mL (for kanamycin), 30 μg/mL (for chloramphenicol), and 100 μg/mL (for ampicillin). For solid medium, 1.5% agar was added.

Generation of Growth Curves. Growth curves were obtained on a Bioscreen C automated growth analysis system. Subcultures of specified strains were grown overnight at 37 °C, diluted in fresh medium at 1:100, inoculated into honeycomb wells in triplicate, and grown at 37 °C with maximum shaking on the platform of the Bioscreen C instrument. When the cultures reached an OD_{600} of 0.2, cells were treated with H_2O_2 (2 mM) and incubated at 37 °C for 10 h. OD_{600} values were recorded automatically at specified times, and the mean value of the triplicate cultures was plotted.

Generation of Survival Curves. Overnight cultures were inoculated into Luria–Bertani broth and grown at 37 °C to ~2×10^7 cells per 1 mL. Cells were then treated with H_2O_2 (2 mM) and after 10 or 20 min of incubation, samples were diluted, plated on Luria–Bertani broth agar, and incubated at 37 °C for 16–18 h. Cell survival was determined by counting cfu and is shown as the mean value ± SD from three independent experiments.

H_2S Detection. To monitor H_2S production, we used a $Pb(Ac)_2$ detection method (14) and the TICT-based fluorescent H_2S probe (BH-HS) (15). Overnight cultures were diluted 1:500 in Luria–Bertani broth and incubated at 37 °C with aeration (250 rpm) for 18–20 or 3–4 h for $Pb(Ac)_2$ or BH-HS, respectively. Before incubation, the paper strips saturated with 2% $Pb(Ac)_2$ were affixed to the inner wall of a cultural tube above the level of the liquid culture of WT or mutant bacteria. Stained paper strips were scanned and quantified with an Alpha Imager (Imgen Technologies). BH-HS (5 μM) was added to liquid bacterial culture, and after 40 min, the aliquots were taken for fluorescent microscopy (API DeltaVision PersonalDV system with Olympus IX-71 inverted microscope base). Images were taken with an Olympus PlanApo N 60×/1.42 oil lens. A Cytation 3 (BioTek Instruments Inc.) was used to quantitate fluorescence. The results were normalized according to the ODs.

Measurement of Luminescent Reaction of Lux Biosensors. The SOS response was examined using a pColD′::lux hybrid plasmid (38), a derivative of the pDEW201 vector containing *lux*CDABE from *Photorhabdus luminescens* under the control of the LexA-regulated *Pcda* promoter (25). Overnight cultures of strains containing the pColD′::lux plasmid were diluted to a concentration of 10^7 cells per 1 mL in fresh Luria–Bertani broth medium and grown under aeration at 30 °C until the early exponential growth phase; 200-μL aliquots were transferred into special cuvettes, one of which served as a control (4 mL distilled water was added to the control cuvette), and 4 mL peroxide was introduced at various concentrations into the other cuvettes. Samples of lux biosensors thus prepared were placed in front of a photomultiplier in an LMAO1 luminometer (Beckman), and the intensity of bioluminescence of the cell suspension was measured at certain times. The samples were incubated at room temperature. The bioluminescence intensity was determined according to ref. 39.

RNA Extraction and qRT-PCR. *E. coli* K-12 MG1655 cells were grown until OD_{600} of 0.6, and total RNA was extracted using the RNeasy Mini Kit (QIAGEN) according to the manufacturer's protocol. All RNA samples were treated with DNaseI (Fermentas); 500 ng total RNA was reverse-transcribed with 100 U SuperScript III enzyme from the First-Strand Synthesis Kit for RT-PCR (Invitrogen) according to the manufacturer's protocol in the presence of appropriate gene-specific primers (Table S2). One microliter reverse transcription reaction was used as the template for real-time PCR. The gene *def* encoding peptide deformylase was used for normalization. Each real-time PCR mixture (25 μL) contained 10 μL SYBR Green I PCR Master Mix (Syntol), 12 μL nuclease-free H_2O, 1 μL 10 μM forward primer, 1 μL 10 μM reverse primer, and 1 μL cDNA template. Amplifications were carried out using the DTlite S1 CyclerSystem (DNA Technology). Reaction products were analyzed using 2% agarose electrophoresis to confirm that the detected signals originated from products of expected lengths. Each qRT-PCR was performed at least in triplicate, and average data are reported. Error bars correspond to the SD.

TUNEL Assay. Cells were grown until OD_{600} of 0.4, and 1-mL aliquots were treated with 5 mM H_2O_2 for 30 min. Cells were fixed and labeled using a slightly modified protocol for the Apo-Direct TUNEL assay kit (EMD Millipore). Briefly, treated cells were harvested, washed, and resuspended in 1 mL cold 4% paraformaldehyde, and then, they were incubated on ice. After 1 h, cells were centrifuged, washed, and resuspended in 70% ethanol overnight at −20 °C. The next day, cells were centrifuged, washed, and resuspended in 50 μL TUNEL reaction mix for 2 h at 37 °C. After the labeling reaction was stopped, the cells were counterstained with propidium iodide/RNase A and analyzed by flow cytometry on the FACSCalibur.

ACKNOWLEDGMENTS. This work was supported by Russian Science Foundation Grants 14-14-00524 (to A.M., V.K., G.Z., and R.S.) and 14-50-00060 (to A.M., T.S., and M.N.), the Blavatnik Family Foundation, and the Howard Hughes Medical Institute (L.G.L., K.S., and E.N.).

1. Kimura H (2014) Production and physiological effects of hydrogen sulfide. *Antioxid Redox Signal* 20:783–793.
2. Shatalin K, Shatalina E, Mironov A, Nudler E (2011) H_2S: A universal defense against antibiotics in bacteria. *Science* 334:986–990.
3. Fu LH, et al. (2014) An antifungal role of hydrogen sulfide on the postharvest pathogens *Aspergillus niger* and *Penicillium italicum*. *PLoS One* 9:e104206.
4. Wu G, Wan F, Fu H, Li N, Gao H (2015) A matter of timing: Contrasting effects of hydrogen sulfide on oxidative stress response in *Shewanella oneidensis*. *J Bacteriol* 197:3563–3572.
5. Awano N, Wada M, Mori H, Nakamori S, Takagi H (2005) Identification and functional analysis of *Escherichia coli* cysteine desulfhydrases. *Appl Environ Microbiol* 71:4149–4152.
6. Datta P (1967) Regulation of homoserine biosynthesis by L-cysteine, a terminal metabolite of a linked pathway. *Proc Natl Acad Sci USA* 58:635–641.
7. Carlsson J, Granberg GP, Nyberg GK, Edlund MB (1979) Bactericidal effect of cysteine exposed to atmospheric oxygen. *Appl Environ Microbiol* 37:383–390.
8. Kredich NM, Tomkins GM (1966) The enzymic synthesis of L-cysteine in Escherichia coli and Salmonella typhimurium. *J Biol Chem* 241:4955–4965.
9. Kredich NM (1992) The molecular basis for positive regulation of *cys* promoters in *Salmonella typhimurium* and *Escherichia coli*. *Mol Microbiol* 6:2747–2753.
10. Park S, Imlay JA (2003) High levels of intracellular cysteine promote oxidative DNA damage by driving the fenton reaction. *J Bacteriol* 185:1942–1950.
11. Imlay JA (2003) Pathways of oxidative damage. *Annu Rev Microbiol* 57:395–418.
12. Kohanski MA, Dwyer DJ, Hayete B, Lawrence CA, Collins JJ (2007) A common mechanism of cellular death induced by bactericidal antibiotics. *Cell* 130:797–810.
13. Zhao X, Drlica K (2014) Reactive oxygen species and the bacterial response to lethal stress. *Curr Opin Microbiol* 21:1–6.
14. Forbes BA (1998) *Bailey and Scott's Diagnostic Microbiology* (Mosby, St. Louis), 10th Ed.
15. Ren M, et al. (2016) A TICT-based fluorescent probe for rapid and specific detection of hydrogen sulfide and its bio-imaging applications. *Chem Commun (Camb)* 52:6415–6418.
16. Imlay JA, Linn S (1986) Bimodal pattern of killing of DNA-repair-defective or anoxically grown *Escherichia coli* by hydrogen peroxide. *J Bacteriol* 166:519–527.
17. Hantke K (2001) Iron and metal regulation in bacteria. *Curr Opin Microbiol* 4:172–177.
18. Hantke K, Braun V (2000) The art of keeping low and high iron concentrations in balance. *Bacterial Stress Responses*, eds Storz G, Hengge-Aronis R (ASM, Washington, DC), pp 275–288.
19. Massé E, Vanderpool CK, Gottesman S (2005) Effect of RyhB small RNA on global iron use in *Escherichia coli*. *J Bacteriol* 187:6962–6971.
20. Touati D, Jacques M, Tardat B, Bouchard L, Despied S (1995) Lethal oxidative damage and mutagenesis are generated by iron in delta *fur* mutants of *Escherichia coli*: Protective role of superoxide dismutase. *J Bacteriol* 177:2305–2314.
21. Keyer K, Imlay JA (1996) Superoxide accelerates DNA damage by elevating free-iron levels. *Proc Natl Acad Sci USA* 93:13635–13640.
22. Keyer K, Gort AS, Imlay JA (1995) Superoxide and the production of oxidative DNA damage. *J Bacteriol* 177:6782–6790.
23. Aruoma OI, Halliwell B, Gajewski E, Dizdaroglu M (1989) Damage to the bases in DNA induced by hydrogen peroxide and ferric ion chelates. *J Biol Chem* 264:20509–20512.
24. Imlay JA, Chin SM, Linn S (1988) Toxic DNA damage by hydrogen peroxide through the Fenton reaction in vivo and in vitro. *Science* 240:640–642.
25. Kotova VY, Manukhov IV, Zavilgelsky GB (2010) Lux-biosensors for detection of SOS-response, heat shock, and oxidative stress. *Appl Biochem Microbiol* 46:781–788.

26. Ohtsu I, et al. (2010) The L-cysteine/L-cystine shuttle system provides reducing equivalents to the periplasm in *Escherichia coli*. *J Biol Chem* 285:17479–17487.
27. Ohtsu I, et al. (2015) Uptake of L-cystine via an ABC transporter contributes defense of oxidative stress in the L-cystine export-dependent manner in *Escherichia coli*. *PLoS One* 10:e0120619.
28. Chonoles Imlay KR, Korshunov S, Imlay JA (2015) Physiological roles and adverse effects of the two cystine importers of *Escherichia coli*. *J Bacteriol* 197:3629–3644.
29. Sezonov G, Joseleau-Petit D, D'Ari R (2007) *Escherichia coli* physiology in Luria-Bertani broth. *J Bacteriol* 189:8746–8749.
30. Zheng M, et al. (2001) DNA microarray-mediated transcriptional profiling of the *Escherichia coli* response to hydrogen peroxide. *J Bacteriol* 183:4562–4570.
31. Luhachack L, Nudler E (2013) H2S as a bacterial defense against antibiotics. *Hydrogen Sulfide and Its Therapeutic Applications*, ed Kimura H (Springer, Vienna), pp 173–180.
32. Luhachack L, Nudler E (2014) Bacterial gasotransmitters: An innate defense against antibiotics. *Curr Opin Microbiol* 21:13–17.
33. Zhao X, Hong Y, Drlica K (2015) Moving forward with reactive oxygen species involvement in antimicrobial lethality. *J Antimicrob Chemother* 70:639–642.
34. Baba T, et al. (2006) Construction of Escherichia coli K-12 in-frame, single-gene knockout mutants: The Keio collection. *Mol Syst Biol* 2:2006.008.
35. Miller JH (1972) *Experiments in Molecular Genetics* (Cold Spring Harbor Lab Press, Cold Spring Harbor, NY).
36. Datsenko KA, Wanner BL (2000) One-step inactivation of chromosomal genes in *Escherichia coli* K-12 using PCR products. *Proc Natl Acad Sci USA* 97:6640–6645.
37. Sambrook J, Fritsch E, Maniatis T (1989) *Molecular Cloning: A Laboratory Manual* (Cold Spring Harbor Lab Press, Cold Spring Harbor, NY), 2nd Ed.
38. Winson MK, et al. (1998) Engineering the *luxCDABE* genes from *Photorhabdus luminescens* to provide a bioluminescent reporter for constitutive and promoter probe plasmids and mini-Tn5 constructs. *FEMS Microbiol Lett* 163:193–202.
39. Zavilgelsky GB, Kotova VY, Manukhov IV (2007) Action of 1,1-dimethylhydrazine on bacterial cells is determined by hydrogen peroxide. *Mutat Res* 634:172–176.
40. Lutz R, Bujard H (1997) Independent and tight regulation of transcriptional units in *Escherichia coli* via the LacR/O, the TetR/O and AraC/I1-I2 regulatory elements. *Nucleic Acids Res* 25:1203–1210.